Inorg. Chem. **2008**, *47*, 8696−8703

Influence of Ligand Polarizability on the Reversible Binding of O_2 by *trans*-[Rh(X)(XNC)(PPh_3)$_2$] (X = Cl, Br, SC_6F_5, C_2Ph; XNC = Xylyl Isocyanide). Structures and a Kinetic Study

Laurence Carlton,* Lebohang V. Mokoena, and Manuel A. Fernandes

Molecular Sciences Institute, School of Chemistry, University of the Witwatersrand, Johannesburg, Republic of South Africa

Received March 17, 2008

The complexes *trans*-[Rh(X)(XNC)(PPh_3)$_2$] (X = Cl, **1**; Br, **2**; SC_6F_5, **3**; C_2Ph, **4**; XNC = xylyl isocyanide) combine reversibly with molecular oxygen to give [Rh(X)(O_2)(XNC)(PPh_3)$_2$] of which [Rh(SC_6F_5)(O_2)(XNC)(PPh_3)$_2$] (**7**) and [Rh(C_2Ph)(O_2)(XNC)(PPh_3)$_2$] (**8**) are sufficiently stable to be isolated in crystalline form. Complexes **2**, **3**, **4**, and **7** have been structurally characterized. Kinetic data for the dissociation of O_2 from the dioxygen adducts of **1**−**4** were obtained using ^{31}P NMR to monitor changes in the concentration of [Rh(X)(O_2)(XNC)(PPh_3)$_2$] (X = Cl, Br, SC_6F_5, C_2Ph) resulting from the bubbling of argon through the respective warmed solutions (solvent chlorobenzene). From data recorded at temperatures in the range 30−70 °C, activation parameters were obtained as follows: $\Delta H^{\ddagger}$ (kJ mol^{-1}): 31.7 ± 1.6 (X = Cl), 52.1 ± 4.3 (X = Br), 66.0 ± 5.8 (X = SC_6F_5), 101.3 ± 1.8 (X = C_2Ph); $\Delta S^{\ddagger}$ (J K^{-1} mol^{-1}): −170.3 ± 5.0 (X = Cl), −120 ± 13.6 (X = Br), −89 ± 18.2 (X = SC_6F_5), −6.4 ± 5.4 (X = C_2Ph). The values of $\Delta H^{\ddagger}$ and $\Delta S^{\ddagger}$ are closely correlated (R^2 = 0.9997), consistent with a common dissociation pathway along which the rate-determining step occurs at a different position for each X. Relative magnitudes of $\Delta H^{\ddagger}$ are interpreted in terms of differing polarizabilities of ligands X.

Introduction

The ability of a transition metal to combine with molecular oxygen is related to the presence of a vacant coordination site, the accessibility of a higher oxidation state, the electron density on the metal and the polarizability of the metal, governed in part by the polarizability of attached ligands. The relative ease with which suitable conditions can be achieved is reflected in the wide range of known O_2 complexes.[1] The influence of metal polarizability on oxygen binding ability is shown by the complexes *trans*-[Ir(Cl)(CO)(PPh_3)$_2$][2] and *trans*-[Rh(Cl)(CO)(PPh_3)$_2$]:[3] the former combines reversibly with O_2, while the latter does not react. The influence of ligand polarizability on O_2 binding is shown by the complexes [Rh(Cl)(PPh_3)$_3$] and [Rh($NCBPh_3$)(PPh_3)$_3$]: the former binds O_2 (irreversibly)[4] while the latter does not.[5] Our interest in transition metal−O_2 interactions arises from work directed toward a fuller understanding of ligand polarizability effects. In the present study we examine the role of the anionic ligand in promoting oxygen binding by the complexes *trans*-[Rh(X)(XNC)(PPh_3)$_2$] (X = Cl, Br, SC_6F_5, C_2Ph; XNC = xylyl isocyanide).

Experimental Section

Materials. [Rh(Cl)(PPh_3)$_3$] and [Rh(Br)(PPh_3)$_3$] were prepared by the method of Wilkinson,[6] and [Rh(H)(PPh_3)$_4$] was prepared by the method of Robinson.[7] Xylyl isocyanide (2,6-dimethylphenyl isocyanide) was purchased from Fluka, and pentafluorophenyl thiol

* To whom correspondence should be addressed. E-mail: laurence.carlton@wits.ac.za.

(1) (a) Choy, V. J.; O'Connor, C. J. *Coord. Chem. Rev.* **1972**, *9*, 145. (b) Valentine, J. S. *Chem. Rev.* **1973**, *73*, 235. (c) Henrici-Olivé, G.; Olivé, S. *Angew. Chem., Int. Ed. Engl.* **1974**, *13*, 29. (d) Vaska, L. *Acc. Chem. Res.* **1976**, *9*, 175. (e) Collman, J. P. *Acc. Chem. Res.* **1977**, *10*, 265. (f) Jones, R. D.; Summerville, D. A.; Basolo, F. *Chem. Rev.* **1979**, *79*, 139. (g) Gubelman, M. H.; Williams, A. F. *Struct. Bonding (Berlin)* **1983**, *55*, 1. (h) Niederhofer, E. C.; Timmons, J. H.; Martell, A. E. *Chem. Rev.* **1984**, *84*, 137. (i) Karlin, K. D.; Gultneh, Y. *Prog. Inorg. Chem.* **1987**, *35*, 219. (j) Dickman, M. H.; Pope, M. T. *Chem. Rev.* **1994**, *94*, 569. (k) Busch, D. H.; Alcock, N. W. *Chem. Rev.* **1994**, *94*, 585. (l) Butler, A.; Clague, M. J.; Meister, G. E. *Chem. Rev.* **1994**, *94*, 625. (m) Momenteau, M.; Reed, C. A. *Chem. Rev.* **1994**, *94*, 659. (n) Kitajima, N.; Moro-oka, Y. *Chem. Rev.* **1994**, *94*, 737. (o) Pecoraro, V. L.; Baldwin, M. J.; Gelasco, A. *Chem. Rev.* **1994**, *94*, 807.

(2) Vaska, L. *Acc. Chem. Res.* **1968**, *1*, 335.
(3) Vallarino, L. J. *Chem. Soc.* **1957**, 2287.
(4) Bennett, M. J.; Donaldson, P. B. *Inorg. Chem.* **1977**, *16*, 1581.
(5) Carlton, L.; Weber, R. *Inorg. Chem.* **1996**, *35*, 5843.

10.1021/ic800478g CCC: $40.75
Published on Web 09/06/2008

and phenylacetylene were purchased from Aldrich Chemicals. Dichloromethane was distilled from P_2O_5. Diethyl ether, 1,2-dichloroethane, hexane, benzene, chlorobenzene, and toluene were dried over calcium hydride. All operations except those involving molecular oxygen were performed under an argon atmosphere.

Preparation of *trans*-[Rh(Cl)(XNC)(PPh_3)$_2$]·(0.5CH_2Cl_2) (1). A mixture of [Rh(Cl)(PPh_3)$_3$] (0.050 g, 0.054 mmol) and xylyl isocyanide (0.007 g, 0.054 mmol) was dissolved in dichloromethane (3 mL) at room temperature. After a few minutes, during which time a color change to orange-red was observed, the solution was concentrated, treated with hexane, and allowed to stand for 20 h at room temperature to give the product as a yellow microcrystalline powder. Yield 0.039 g (84%). ^{1}H NMR (chloroform 300 K) δ 7.81−7.73 (mult, 12H, Ar), 7.26−7.20 (mult, Ar, 18 H), 6.79 (t (J = 7.8), 1H, XNC Ar-4), 6.67 (d (J = 7.8), 2H, XNC Ar-3,5), 1.61 (s, 6H, XNC Me); ^{31}P NMR (dichloromethane 300 K) δ 30.80 (d J(^{103}Rh, ^{31}P) 135 Hz); ^{103}Rh NMR (dichloromethane 300 K) δ −261 ppm. Anal. Calcd for **1**: C, 63.57; H, 4.69; N, 1.63. Found: C, 64.06; H, 4.53; N, 1.69.

Preparation of *trans*-[Rh(Br)(XNC)(PPh_3)$_2$]·(0.5CH_2Cl_2) (2). A mixture of [Rh(Br)(PPh_3)$_3$] (0.100 g, 0.103 mmol) and xylyl isocyanide (0.014 g, 0.108 mmol) was dissolved in dichloromethane (4 mL) at room temperature. After a few minutes, during which time a color change to dark red was observed, the solution was centrifuged to remove a small quantity of black powder, concentrated, treated with hexane, and allowed to stand for 20 h at room temperature to give the product as a yellow crystalline powder. Yield 0.059 g (62%). ^{1}H NMR (benzene 300 K) δ 8.14−8.02 (mult, 12H, Ar), 7.05−6.86 (mults, 18H Ar), 6.60 (t (J = 7.3), 1H, XNC Ar-4), 6.48 (d (J = 7.3), 2H, XNC Ar-3,5), 1.62 (s, 6H, XNC Me); ^{31}P NMR (toluene 300 K) δ 31.40 (d J(^{103}Rh, ^{31}P) 134 Hz); ^{103}Rh NMR (toluene 300 K) δ −325 ppm. Anal. Calcd for $C_{45.5}H_{40}ClBrNP_2Rh$: C, 62.03; H, 4.58; N, 1.59. Found: C, 62.33; H, 5.00; N, 1.84. In addition to **2**, a small quantity of red-brown crystals of [Rh(Br)$_3$(XNC)(PPh_3)$_2$](CH_2Cl_2) (**2b**) was also obtained from solutions allowed to stand for more than 1 d.

Preparation of *trans*-[Rh(SC_6F_5)(XNC)(PPh_3)$_2$]·(0.5 Et_2O) (3). A stirred suspension of [Rh(H)(PPh_3)$_4$] (0.150 g, 0.130 mmol) in Et_2O (3 mL) at room temperature was treated first with C_6F_5SH (0.030 g, 0.150 mmol) followed by, after 1−2 min when a clear orange solution had been obtained, xylyl isocyanide (0.017 g, 0.130 mmol). After a further 5 min, stirring was discontinued and the solution was allowed to stand for 20 h at room temperature to give the product as yellow crystals. Yield 0.096 g (74%). ^{1}H NMR (benzene 300 K) δ 8.00−7.92 (mult, 12H, Ar), 7.02−6.88 (mult, 18H, Ar), 6.55 (t (J = 7.5), 1H, XNC Ar-4), 6.43 (d (J = 7.5), 2H, XNC Ar-3,5), 1.60 (s, 6H, XNC Me); ^{31}P NMR (toluene 300 K) δ 32.53 (dt J(^{103}Rh, ^{31}P) 139, J(^{31}P, ^{19}F) 3.1 Hz); ^{103}Rh NMR (toluene 300 K) δ −366 ppm. Anal. Calcd for $C_{53}H_{44}F_5NO_{0.5}P_2RhS$: C, 63.99; H, 4.46; N, 1.41. Found: C, 64.11; H, 4.20; N, 1.47.

Preparation of *trans*-[Rh(C_2Ph)(XNC)(PPh_3)$_2$]·(C_6H_6) (4). [Rh(H)(PPh_3)$_4$] (0.048 g, 0.042 mmol) and PhC_2H (0.010 g 0.10 mmol) were allowed to combine (with stirring) at room temperature in benzene (2 mL), distilled under vacuum from CaH_2 into the reaction flask. Within 2−3 min a dark red solution was obtained. After stirring for ∼10 min, xylyl isocyanide (0.0055 g, 0.042 mmol) was added and stirring was continued for a further 15 min. The solution was then concentrated, treated with hexane, and allowed to stand at room temperature for 2 d to give the product as yellow crystals. Yield 0.022 g (56%). ^{1}H NMR (benzene 300 K) δ 8.18−8.12 (mult, 12H, Ar), 7.06−6.88 (mults, 20H, Ar), 6.84−6.77 (mult, 3H, Ar), 6.62 (t (J = 7.3), 1H, XNC Ar-4), 6.51 (d (J = 7.3), 2H, XNC Ar-3,5),1.60 (s, 6H, XNC Me); ^{31}P NMR (toluene 300 K) δ 35.82 (d J(^{103}Rh, ^{31}P) 144 Hz); ^{103}Rh NMR (toluene 300 K) δ −687 ppm. Anal. Calcd for $C_{59}H_{50}NP_2Rh$: C, 75.56; H, 5.37; N.1.49. Found: C, 75.95; H, 5.86; N, 1.67.

Reaction of 1 with O_2. On shaking a solution of **1** in dichloromethane with O_2 [Rh(Cl)(O_2)(XNC)(PPh_3)$_2$] (**5**) was obtained (72% conversion measured by ^{31}P NMR). IR (dichloromethane) ν(O_2) 894 (m, br) cm^{-1}; ^{1}H NMR (chloroform 300 K) δ 7.69−7.63 (mult, 12H, Ar), 7.36−7.22 (mults, 18H, Ar), 7.02 (t (J = 7.5), 1H, XNC Ar-4), 6.89 (d (J = 7.5), 2H, XNC Ar-3, 5), 1.99 (s, 6H XNC Me); ^{31}P NMR (dichloromethane 300 K): δ 28.14 (d J(^{103}Rh, ^{31}P) 91 Hz); ^{103}Rh NMR (dichloromethane 300 K) δ 2130 ppm. Attempts to isolate **5** yielded only **1**.

Reaction of 2 with O_2. On shaking a solution of **2** in toluene with O_2 [Rh(Br)(O_2)(XNC)(PPh_3)$_2$] (**6**) was obtained (100% conversion measured by ^{31}P NMR). IR (dichloromethane) ν(O_2) 894 (m, br) cm^{-1}; ^{1}H NMR (benzene 300 K) δ 8.08−8.00 (mult, 12H, Ar), 7.02−6.93 (mults, 18H, Ar), 6.61 (t (J = 7.5), 1H, XNC Ar-4), 6.49 (d (J = 7.5), 2H, XNC Ar-3,5), 1.96 (s, 6H XNC Me); ^{31}P NMR (toluene 300 K): δ 28.30 (d J(^{103}Rh, ^{31}P) 92 Hz); ^{103} Rh NMR (toluene 300 K) δ 1831 ppm. Attempts to isolate **6** yielded only **2**.

Preparation of [Rh(SC_6F_5)(O_2)(XNC)(PPh_3)$_2$]·(tol). (7). A solution of **3** (0.009 g, 9 mmol) in toluene (1 mL) was shaken with O_2 and allowed to stand for 5 d at −20 °C to give the product as dark brown crystals. Yield 0.007 g (71%). IR (dichloromethane) ν(O_2) 884 (m, br); ^{1}H NMR (benzene 300 K) δ 7.98−7.88 (mult, 12H, Ar), 7.05−6.95 (mults, 18H, Ar), 6.60 (t (J = 7.7), 1H, XNC Ar-4), 6.48 (d (J = 7.7), 2H, XNC Ar-3,5), 2.02 (s, 6H, XNC Me); ^{31}P NMR (toluene 300 K) δ 25.42 (d J(^{103}Rh, ^{31}P) 94 Hz); ^{103}Rh NMR (toluene 300 K) δ 1601 ppm. Anal. Calcd for $C_{58}H_{47}F_5NO_2P_2RhS$: C, 64.39; H, 4.38; N, 1.29. Found: C, 64.96; H, 4.48; N, 1.27.

Preparation of [Rh(C_2Ph)(O_2)(XNC)(PPh_3)$_2$] (8). A solution of **4** (0.010 g, 11 mmol) in benzene (1 mL) was shaken with O_2 and allowed to stand at room temperature for 3 d to give the product as a pink microcrystalline powder. Yield 0.006 g (63%). IR (dichloromethane) ν(O_2) 858 (m, br); ^{1}H NMR (benzene 300 K) δ 8.16−8.07 (mult, 12H, Ar), 7.10−6.90 (mults, 23H, Ar), 6.64 (t (J = 7.6), 1H, XNC Ar-4), 6.51 (d (J = 7.6), 2H, XNC Ar-3,5), 1.87 (s, 6H, XNC Me); ^{13}C NMR (dichloromethane 300 K) acetylide δ 112.28 (dt {^2J(Rh,C) 8.2, J(P,C) 2.4} Rh−Cβ), 100.65 (dt {^1J(Rh,C) 47.3, J(P,C) 15.9} RhCα); ^{31}P NMR (toluene 300 K) δ 31.11 (d J(^{103}Rh, ^{31}P) 92 Hz). ^{103}Rh NMR (toluene 300 K) δ 1010 ppm. Anal. Calcd for $C_{53}H_{44}NO_2P_2Rh$: C, 71.38; H, 4.97; N, 1.57. Found: C, 71.09; H, 5.07; N, 1.50.

NMR Spectroscopy. Spectra were recorded on a Bruker DRX 400 spectrometer equipped with a 5 mm triple resonance inverse probe with a dedicated ^{31}P channel and extended decoupler range operating at 161.98 MHz (^{31}P) and 12.65 MHz (^{103}Rh). Two-dimensional ^{103}Rh−^{31}P spectra were obtained using the pulse sequence $\pi/2(^{31}P)$-1/[$^2J(^{103}Rh,^{31}P)$]-$\pi/2(^{103}Rh)$-τ-$\pi(^{31}P)$-τ-$\pi/2(^{103}Rh)$-1/[$^2J(^{103}Rh,^{31}P)$]-Acq (^{31}P).[8] Further details are given in ref 9. Chemical shifts were referenced to the generally accepted standards of 85% H_3PO_4 and 3.16 MHz (^{103}Rh).[10] The chemical shift of H_3PO_4 (with toluene-d_8 external lock, temperature 300 K) corre-

(6) Osborn, J. A.; Wilkinson, G. *Inorg. Synth.* **1967**, *10*, 67.
(7) Ahmad, N.; Levison, J. J.; Robinson, S. D.; Uttley, M. F. *Inorg. Synth.* **1974**, *15*, 58.
(8) Bax, A.; Griffey, R. H.; Hawkins, B. L. *J. Magn. Reson.* **1983**, *55*, 301.
(9) Carlton, L. *Magn. Reson. Chem.* **2004**, *42*, 760.
(10) Kidd, R. G.; Goodfellow, R. J. In *NMR and the Periodic Table*; Harris, R. K.; Mann, B. E., Eds.; Academic Press: London, 1978; pp 244−249.

Table 1. Crystal Data and Structure Refinement for **2**, **3**, **4**, and **7**

	[Rh(Br)(XNC)(PPh$_3$)$_2$] (CH$_2$Cl$_2$) (**2**)	[Rh(SC$_6$F$_5$)(XNC)(PPh$_3$)$_2$] (0.5 Et$_2$O) (**3**)	[Rh(C$_2$Ph)(XNC)(PPh$_3$)$_2$] (C$_6$H$_6$) (**4**)	[Rh(SC$_6$F$_5$)(O$_2$)(XNC)-(PPh$_3$)$_2$](tol) (**7**)
empirical formula	$C_{46}H_{41}BrCl_2NP_2Rh$	$C_{53}H_{44}F_5NO_{0.5}P_2RhS$	$C_{59}H_{50}NP_2Rh$	$C_{58}H_{47}F_5NO_2P_2RhS$
formula weight	923.46	994.80	937.85	1081.88
temperature (*K*)	173(2)	173(2)	173(2)	173 (2)
wavelength (Å)	0.71073	0.71073	0.71073	0.71073
crystal system	monoclinic	triclinic	triclinic	monoclinic
space group	$P2_1/m$	$P\bar{1}$	$P\bar{1}$	$P2_1/c$
unit cell dimensions	a = 12.1403(10) Å	a = 13.3062 (16) Å	a = 12.481(2) Å	a = 12.9718(16) Å
	b = 12.9180(10) Å	b = 13.5965 (16) Å	b = 13.973(2) Å	b = 14.3791 (15) Å
	c = 12.3376 (9) Å	c = 15.0540 (18) Å	c = 15.361 (3) Å	c = 26.873 (3) Å
	α = 90°	α = 69.599 (2)°	α = 94.931 (3)°	α = 90°
	β = 91.262 (4)°	β = 77.881 (2)°	β = 100.906(3)°	β = 91.497 (4)°
	γ = 90°	γ = 64.300(2)°	γ = 113.722(3)°	γ = 90°
volume (Å^3)	1934.4(3)	2294.6(5)	2368.8(7)	5010.8(10)
Z	2	2	2	4
density (calculated) (Mg/m^3)	1.585	1.440	1.315	1.434
absorption coefficient (mm^{-1})	1.731	0.547	0.468	0.509
crystal size (mm^3)	0.26 × 0.24 × 0.03	0.38 × 0.26 × 0.09	0.26 × 0.20 × 0.07	0.17 × 0.16 × 0.06
θ range for data collection (deg)	2.28 to 28.27	1.45 to 27.00	1.37 to 27.00	1.52 to 27.00
index ranges	$-15 \le h \le 16$	$-16 \le h \le 13$	$-15 \le h \le 15$	$-16 \le h \le 12$
	$-17 \le k \le 17$	$-17 \le k \le 17$	$-17 \le k \le 15$	$-18 \le k \le 18$
	$-14 \le l \le 16$	$-18 \le l \le 19$	$-19 \le l \le 19$	$-32 \le l \le 34$
reflections collected	10584	14651	16013	21943
independent reflections	4986 [R(int) = 0.0520]	9845 [R(int) = 0.0240]	10284 [R(int) = 0.0480]	10680 [R(int) = 0.0768]
completeness to θ_{max} (%)	99.6	98.4	99.4	97.5
max. and min. transmission	0.9481 and 0.6741	0.9524 and 0.8192	0.9721 and 0.8942	0.9636 and 0.9196
data/restraints/parameters	4986/3/261	9845/36/597	10284/1/490	10680/0/619
goodness-of-fit on F^2	1.083	1.010	1.022	0.898
final R indices [$I > 2\sigma(I)$]	R1 = 0.0557	R1 = 0.0310	R1 = 0.0534	R1 = 0.0463
	wR2 = 0.01579	wR2 = 0.0721	wR2 = 0.1368	wR2 = 0.0804
R indices (all data)	R1 = 0.0785	R1 = 0.0496	R1 = 0.0923	R1 = 0.1092
	wR2 = 0.1697	wR2 = 0.0785	wR2 = 0.1565	wR2 = 0.0936
largest diff. peaks (e Å^{-3})	3.598 and −2.449	0.389 and −0.394	1.169 and −0.732	0.656 and −0.728

sponds to a frequency of 161.975488 MHz in a field (9.395 T) in which the protons of tetramethylsilane (TMS, in toluene at 300 K) resonate at 400.130011 MHz.

X-ray Structure Determination. Intensity data were collected at −100 °C on a Bruker SMART 1K CCD area detector diffractometer with graphite-monochromated Mo Kα radiation (50 kV, 30 mA). The collection method involved ω-scans of width 0.3°. Data reduction was carried out using the program SAINT+[11] and face-indexed absorption corrections were made using the program XPREP.[11] The crystal structures (Table 1) were solved by direct methods using SHELXTL.[12] Non-hydrogen atoms were first refined isotropically followed by anisotropic refinement using full-matrix least-squares calculation based on F^2 using SHELXTL. Hydrogen atoms were first located in the difference map and then positioned geometrically and allowed to ride on their respective parent atoms. Diagrams were generated using SHELXTL and PLATON.[13]

In the case of [Rh(C$_2$Ph)(XNC)(PPh$_3$)$_2$].(C$_6$H$_6$) (**4**) both the phenylacetylide ligand and the cocrystallized benzene are disordered. Each was refined over two positions with site occupancies set to 0.5; the refinement of the phenylacetylide ligand, however, can not be regarded as optimal. Attempts to improve crystal quality by using dichloromethane, toluene, or diethylether as the growth medium were unsuccessful. In addition crystal shattering occurred at temperatures below −100 °C, preventing the collection of improved data.

Kinetic Study. Reactions were carried out in a 5 mm NMR tube and changes in concentration monitored by ^{31}P NMR. In each experiment the starting material {*trans*-[Rh(X)(XNC)(PPh$_3$)$_2$], sufficient to give a ∼0.02 M solution with 0.5 mL of solvent}, was placed in an NMR tube; the solvent, 0.5 mL chlorobenzene containing 5 drops of toluene-d$_8$, was added under argon and warmed to dissolve the solid. The solution was then cooled, and oxygen gas was admitted into the tube which was shaken (10−20 s) until complete conversion of the starting material to the dioxygen complex (72% in the case X = Cl) was obtained, as shown by the ^{31}P spectrum. A sealed capillary (length ∼10 cm, external diameter ∼1.5 mm) containing Me$_3$PO$_4$ was then admitted into the tube for the purpose of calibrating the ^{31}P signal (peak height). A ^{31}P reference spectrum (time zero) was then recorded. The NMR tube was then transferred to a bath maintained at a constant temperature in the range 30−70 °C. The tube was immersed to a depth of ∼ 5−6 cm, that is, to a level exceeding that of the contents. Simultaneously, by means of a capillary, argon was bubbled through the solution at a predetermined rate of 3.2 ± 0.1 mL min^{-1}. After a measured interval, which varied in duration from 10 s to 5 min depending upon the complex and the temperature, the heating and bubbling of argon were simultaneously discontinued and the reaction was rapidly quenched in an ice−water mixture. During this time (10−15 s) argon was allowed to flow into the NMR tube which was then sealed prior to the recording of a ^{31}P spectrum (128 scans). This process, from transfer to the bath to the recording of a spectrum, was repeated a number (in the range 5−12) of times. Where necessary, allowance was made for small losses of solvent by evaporation at higher temperatures.

The ^{31}P signal heights were calibrated against the Me$_3$PO$_4$ signal for each spectrum and converted into concentrations by comparison with the initial spectrum (t = 0) in the series. A first order rate constant for the dissociation of O$_2$ was obtained from a plot of ln{concentration of [Rh(X)(O$_2$)(XNC)(PPh$_3$)$_2$]} against time. No significant difference in rate was found on changing the solvent to

(11) *SAINT*+, Version 6.02 (includes XPREP); Bruker AXS, Inc.: Madison, WI, 1999.
(12) *SHELXTL*, Version 5.1; Bruker AXS, Inc.: Madison, WI, 1999.
(13) Spek, A. L. *J. Appl. Crystallogr.* **2003**, *36*, 7.

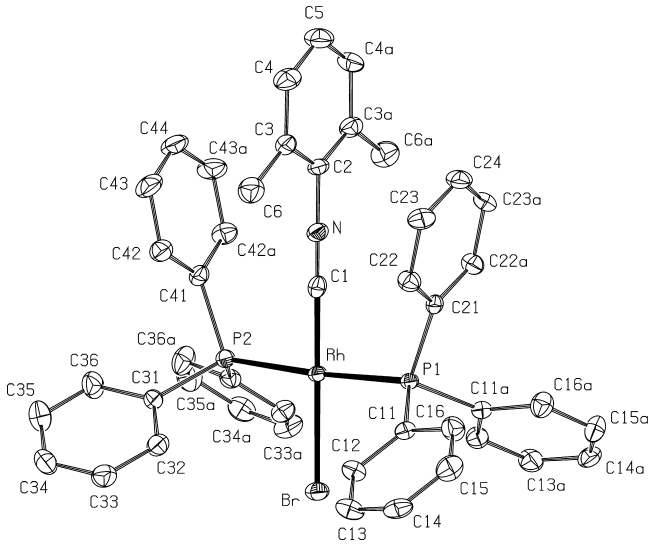

Figure 1. Diagram of *trans*-[Rh(Br)(XNC)(PPh_3)$_2$] (**2**). Thermal ellipsoids are shown at the 50% probability level. Hydrogens and a cocrystallized CH_2Cl_2 are omitted.

1,2-dichloroethane or of a decrease (10%) in the rate of bubbling of argon. Using the Eyring equation $\{\ln(k_1h/k_BT) = -(\Delta H^{\ddagger}/R)(1/T) + \Delta S^{\ddagger}/R$; k_1 = observed rate, k_B = Boltzmann constant, h = Planck's constant, R = gas constant$\}$ a plot of $\ln(k_1h/k_BT)$ versus $1/T$ gave the dissociation enthalpy and entropy from the gradient and intercept, respectively.

Results and Discussion

Complexes. The complexes *trans*-[Rh(X)(XNC)(PPh_3)$_2$] (X = Cl, **1**; Br, **2**; SC_6F_5, **3**; C_2Ph, **4**; XNC = 2,6-dimethylphenyl isocyanide, xylyl isocyanide) are obtained in moderate to good yield by the reaction of [Rh(X)(PPh_3)$_3$] (X = Cl, Br) with XNC and by the reaction of [Rh(H)(PPh_3)$_4$] with RH (R = C_6F_5S, C_2Ph) followed by XNC. On slowly crystallizing **2** (X = Br) small quantities of [Rh(Br)$_3$(XNC)(PPh_3)$_2$] (**2b**) are obtained. In solution complexes **1**−**4** bind dioxygen reversibly, but only in the case of **3** and **4** can O_2 adducts {[Rh(SC_6F_5)(O_2)(XNC)(PPh_3)$_2$] (**7**) and [Rh(C_2Ph)(O_2)(XNC)(PPh_3)$_2$] (**8**)} be isolated. Complexes **3** and **4** are air-sensitive in the solid state, **4** significantly more so than **3**. The oxygenated complexes [Rh(Cl)(O_2)(XNC)(PPh_3)$_2$] (**5**) and [Rh(Br)(O_2)(XNC)(PPh_3)$_2$] (**6**) in solution give up O_2 readily, being ∼50% reconverted to **1** and **2** on bubbling argon for 20 s and 3 min, respectively, at 27 °C. For **7** and particularly **8** the process is much slower and heating is required.

Structures. The structures of complexes *trans*-[Rh(X)(XNC)(PPh_3)$_2$], **2** (X = Br), **3** (X = SC_6F_5), and **4** (X = C_2Ph), which exhibit slight distortions from a square planar geometry, are shown in Figures 1−3, respectively. Selected bond lengths and angles are given in Table 2. The most noteworthy feature of the data is a change in the Rh−C(1) (isocyanide) bond length, which increases in the order X = Br < SC_6F_5 < C_2Ph. When the range is extended to include the complex *trans*-[Rh(Cl)(XNC)(P^iPr_3)$_2$], reported by Jones and Hessell,[14] the sequence of Rh-isocyanide carbon bond lengths

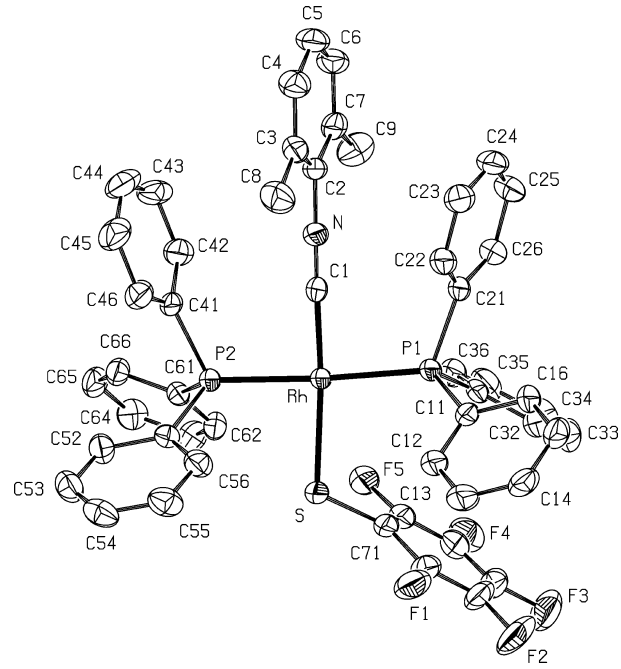

Figure 2. Diagram of *trans*-[Rh(SC_6F_5)(XNC)(PPh_3)$_2$] (**3**). Thermal ellipsoids are shown at the 50% probability level. Hydrogens and a cocrystallized Et_2O are omitted.

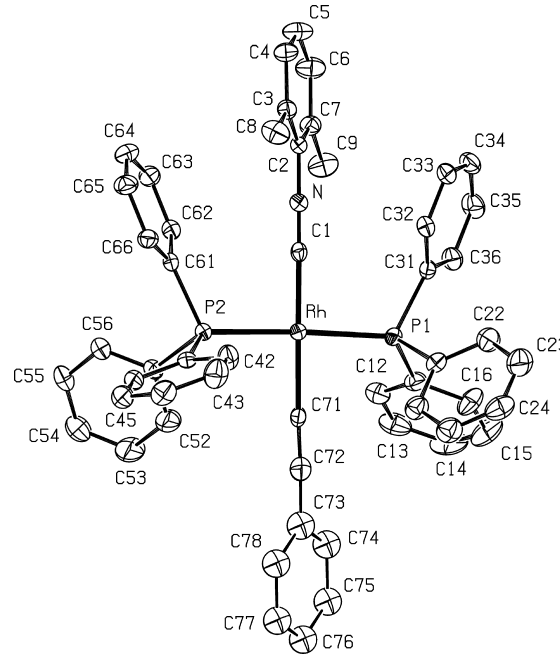

Figure 3. Diagram of *trans*-[Rh(C_2Ph)(XNC)(PPh_3)$_2$] (**4**). Thermal ellipsoids are shown at the 30% probability level. Hydrogens and a cocrystallized benzene are omitted.

(in Å) is as follows: 1.830(5) (X = Cl), 1.861(7) (X = Br), 1.882(2) (X = SC_6F_5), 1.903(4) (X = C_2Ph). This result would appear to arise from the operation of the well-known *trans* influence,[15] a ground-state effect by which metal−ligand interactions are optimized. The polarization process discussed below (which occurs only when the metal interacts with a

(14) Jones, W. D.; Hessell, E. T. *Organometallics* **1990**, *9*, 718.

(15) Appleton, T. G.; Clark, H. C.; Manzer, L. E. *Coord. Chem. Rev.* **1973**, *10*, 335.

Table 2. Selected Bond Lengths (Å) and Angles (deg) for **2**, **3**, and **4**

	[Rh(Br)(XNC)(PPh$_3$)$_2$](CH$_2$Cl$_2$) (**2**)	[Rh(SC$_6$F$_5$)(XNC)(PPh$_3$)$_2$](0.5 Et$_2$O) (**3**)	[Rh(C$_2$Ph)(XNC)(PPh$_3$)$_2$](C$_6$H$_6$) (**4**)
Rh−P(1)	2.3384(18)	2.3227(6)	2.3063(11)
Rh−P(2)	2.3349(18)	2.3349(6)	2.3166(11)
Rh−C(1)	1.861(7)	1.882(2)	1.903(4)
C(1)-N	1.168(9)	1.167(3)	1.184(5)
N−C(2)	1.403(8)	1.401(3)	1.389(5)
Rh−A[a]	2.5196(8)	2.4025(6)	2.030(4)
A−B[b]		1.766(2)	1.298(7)
P(1)−Rh−C(1)	88.1(2)	87.22(6)	91.81(12)
P(1)−Rh−A[a]	91.98(5)	97.23(2)	86.83(13)
P(1)−Rh−P(2)	176.04(6)	175.98(2)	175.61(4)
P(2)−Rh−C(1)	87.9(2)	88.95(6)	91.36(12)
P(2)−Rh−A[a]	91.98(5)	86.55(2)	90.25(13)
C(1)−Rh−A[a]	179.9(2)	174.97(6)	175.3(2)
Rh−A−B[a,b]		113.87(8)	164.8(5)
Rh−C(1)−N	179.6(6)	178.4(2)	177.6(3)

[a] A = bromine (**2**), sulfur (**3**), carbon C (71) (**4**). [b] B = carbon C (71) (**3**), carbon C (72) (**4**).

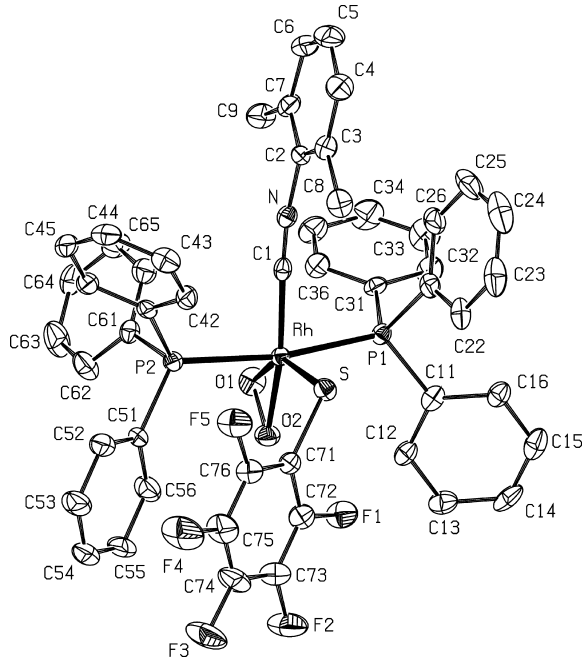

Figure 4. Diagram of [Rh(SC$_6$F$_5$)(O$_2$)(XNC)(PPh$_3$)$_2$] (**7**). Thermal ellipsoids are shown at the 50% probability level. Hydrogens and a cocrystallized toluene are omitted.

reagent, e.g. O_2) can be regarded as occurring independently of this.

The structure of the dioxygen complex [Rh(SC$_6$F$_5$)(O$_2$)(XNC)(PPh$_3$)$_2$] (**7**) is shown in Figure 4 and selected bond lengths and angles are given in Table 3. The geometry is best described as distorted octahedral, the distortions arising from constraints imposed by the O−O bond. Data for **7** are very similar to data for [Rh(CN)(O$_2$)(XNC)(PPh$_3$)$_2$],[16] [Rh(SPh)(O$_2$)(PMe$_3$)$_3$],[17] and [Rh(Cl)(O$_2$)(PPh$_3$)$_3$].[4] The O−O bond length in **7** lies midway between the values found for the Cl and SPh complexes, and for all four complexes there is a close contact between one (or both) of the oxygen atoms and a phenyl hydrogen. In the case of **7** the interaction (2.60 Å) is between O(1) and the hydrogen on C(6) of the isocyanide phenyl of a neighboring molecule.

Kinetic Study. From rate constants measured at temperatures in the range 30−70 °C for the reaction shown in Scheme 1 activation parameters (Table 4) were obtained which show appreciable variation according to ligand X. For the complex showing the fastest rates of dissociation (X = Cl) a fairly small $\Delta H^{\ddagger}$ (31.7 ± 1.6 kJ mol^{-1}) is found together with a large negative $\Delta S^{\ddagger}$ (−170.3 ± 5.0 J K^{-1} mol^{-1}) while for the complex showing the slowest rates (X = C$_2$Ph) a

Table 3. Selected Bond Lengths(Å) and Angles (deg) for [Rh(SC$_6$F$_5$)(O$_2$)(XNC)(PPh$_3$)$_2$] (tol) (**7**)

Rh−P(1)	2.3737(10)	P(1)−Rh−O(2)	95.45 (7)
Rh−P(2)	2.3624(10)	P(1)−Rh−P(2)	167.89(3)
Rh−C(1)	1.939(4)	P(2)−Rh−C(1)	89.99(10)
C(1)−N	1.165(4)	P(2)−Rh−S	98.95(3)
N−C(2)	1.408(4)	P(2)−Rh−O(1)	85.90(8)
Rh−S	2.4226(9)	P(2)−Rh−O(2)	87.72(7)
S−C(71)	1.771(4)	C(1)−Rh−O(1)	120.65(12)
Rh−O(1)	2.044(2)	C(1)−Rh−O(2)	162.01(12)
Rh−O(2)	2.018(2)	C(1)−Rh−S	91.74 10)
O(1)−O(2)	1.436(3)	S−Rh−O(1)	147.37(8)
P(1)−Rh−C(1)	83.38(10)	S−Rh−O(2)	106.24(7)
P(1)−Rh−S	91.40(3)	O(1)−Rh−O(2)	41.39(9)
P(1)−Rh−O(1)	88.77(7)	Rh−O(1)−O(2)	68.35(14)
		Rh−O(2)−O(1)	70.26(14)

Scheme 1. X = Cl (**1**,**5**), Br (**2**,**6**), SC$_6$F$_5$ (**3**,**7**), C$_2$Ph (**4**,**8**); XNC = xylyl isocyanide; P = PPh$_3$; solvent, chlorobenzene

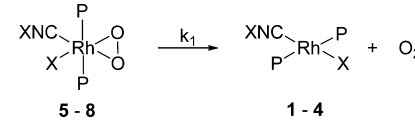

Table 4. Kinetic and Activation Parameters for the Dissociation of O$_2$ from [Rh(X)(O$_2$)(XNC)(PPh$_3$)$_2$] (X = Cl, **5**; Br, **6**; SC$_6$F$_5$, **7**; C$_2$Ph, **8**; XNC = xylyl isocyanide) in Chlorobenzene

ligand X	T/°C	k/s^{-1}	R^{2a}	$\Delta H^{\ddagger}$/kJ mol^{-1}	$\Delta S^{\ddagger}$/J K mol^{-1b}
Cl	30	0.028	0.9951	31.7 ± 1.6	−170.3 ± 5.0
	40	0.042			
	50	0.068			
	60	0.093			
Br	30	0.0041	0.986	52.1 ± 4.3	−119.5 ± 13.6
	40	0.0069			
	50	0.0135			
	60	0.029			
SC$_6$F$_5$	30	0.00065	0.985	66.0 ± 5.8	−88.8 ± 18.2
	40	0.0015			
	50	0.0028			
	60	0.0081			
C$_2$Ph	40	0.00004	0.9997	101.3 ± 1.8	−6.4 ± 5.4
	50	0.00013			
	70	0.0013			

[a] R^2 = correlation coefficient for the plot (not shown) of ln(k_1h/k_BT) vs ($1/T$). [b] $\Delta G^{\ddagger}$ (300 K)/kJ mol^{-1}: Cl, 82.8; Br, 88.0; SC$_6$F$_5$, 92.6; C$_2$Ph, 103.2.

(16) Cîrcu, V.; Fernandes, M. A.; Carlton, L. *Polyhedron* **2002**, *21*, 1775.
(17) Osakada, K.; Hataya, K.; Yamamoto, T. *Inorg. Chem.* **1993**, *32*, 2360.

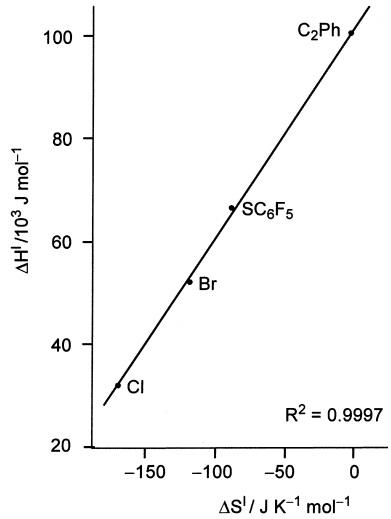

Figure 5. Plot of $\Delta H^{\ddagger}$ vs $\Delta S^{\ddagger}$ for the dissociation of O_2 from [Rh(X)(O_2)(XNC)(PPh_3)$_2$] (X = Cl, **5**; Br, **6**; SC_6F_5, **7**; C_2Ph, **8**) in chlorobenzene.

much larger $\Delta H^{\ddagger}$ is found (101.3 ± 1.8 kJ mol^{-1}) associated with a $\Delta S^{\ddagger}$ close to zero (−6.4 ± 5.4 J K^{-1} mol^{-1}). A plot of $\Delta H^{\ddagger}$ versus $\Delta S^{\ddagger}$ (Figure 5) shows an excellent correlation indicating that, to a high probability, the rate-determining steps for the dissociation of O_2 from the four complexes [Rh(X)(O_2)(XNC)(PPh_3)$_2$] correspond to successive positions along a single generalized reaction coordinate. In such a model the rate-determining step for the chloro complex appears early on the reaction coordinate, where the molecular geometry has undergone few distortions, and the rate-determining step for the acetylide complex appears much later on the reaction coordinate where substantial distortion has occurred. The finding of a negative activation entropy for a reaction involving the evolution of a gas is unusual and would require a highly ordered transition state (see below) but is not unprecedented. For example, an entropy of activation of −41.8 J K^{-1} mol^{-1} has been reported by Vaska and co-workers[18] for the dissociation of O_2 from [Ir(NCO)(O_2)(PPh_3)$_2$(CO)] (see below). A correlation between enthalpy and entropy of activation is frequently encountered in weakly bonded interactions.[19] A possible explanation for the results shown in Figure 5 is as follows. The requirement of a highly ordered transition state is met by a situation in which the metal−ligand bonds all vibrate in unison, that is, they simultaneously stretch and simultaneously shrink, with the result that electron density in the metal-dioxygen bond(s) is depleted to the greatest possible extent when the metal−ligand bonds experience maximum extension. The differing contributions of electron density from ligands X, in particular contributions arising from electron density normally residing on the ligand (polarizability effects), will then govern the position of the rate-determining step on the reaction coordinate.

(18) Vaska, L.; Chen, L. S.; Senoff, C. V. *Science* **1971**, *174*, 587.

(19) (a) Williams, D. H.; Searle, M. S.; Westwell, M. S.; Gerhard, U.; Holroyd, S. E. *Phil. Trans. R. Soc. Lond. Ser. A.* **1993**, *354*, 11. (b) Searle, M. S.; Westwell, M. S.; Williams, D. H. *J. Chem. Soc., Perkin Trans. 2* **1995**, 141. (c) Williams, D. H.; Westwell, M. S. *Chem. Soc. Rev.* **1998**, *27*, 57.

The work of Williams and co-workers[19] has provided a broad perspective of enthalpy−entropy relationships in weakly bonded systems. A part of this account is summarized briefly here. In a weak molecular association, where the binding enthalpy is much lower than that of typical covalent bonds, the potential energy well corresponding to the associated state is shallow. Such a molecular association has much residual motion (unlike the associated state occupying a deep well) since energy levels corresponding to large amplitude vibrations close to the lip of the well will be more highly populated than when the well is deep. Weak associations with small binding enthalpies can give rise to remarkably small losses of entropy (upon binding), and the limiting entropy, corresponding to the maximum possible loss of motion, is only likely to be achieved in the case of a very large binding enthalpy (a deep potential well).

Results reported in the present study can be interpreted in this context. If, in a weakly associated system (such as a metal−O_2 complex), where the loss of entropy relative to the isolated components (here the metal complex and free molecular oxygen) is not large, the route to dissociation lies through a small number of vibrational modes (or even a single vibrational mode), then the transfer of vibrational energy from the many modes (corresponding to the high density of populated states close to the lip of the potential well) to the very much smaller number of modes that can lead to dissociation will involve the creation of order out of relative disorder. A negative entropy can be expected for such a process, with magnitude related to the shallowness of the well and to the density of states close to the lip. For more strongly associated systems (metal−O_2 complexes having higher $\Delta H^{\ddagger}$) with a deeper potential well the opportunities for vibrational motion will be more restricted and the redistribution of vibrational energy that will be required prior to dissociation will be proportionally less, involving a smaller (less negative) activation entropy. Williams[19b] draws attention to the number of studies that have shown a linear relationship between the binding enthalpy and the entropy change in the formation of weakly bonded molecular associations.

A possible precedent for a rhodium−dioxygen complex in which the O_2 has high residual motion can be found in a recent report by Milstein and co-workers.[20] The complex [{$Me_2C_6H(CH_2P^tBu_2)_2$}Rh(η^2-O_2)] has an unusually short O−O bond (1.365(18)Å), a value of J(^{103}Rh, ^{31}P) of 146 Hz, indicative more of Rh(I) than Rh(III), and readily gives up O_2 in exchange for CO. The authors interpret this evidence in terms of an interaction of the type

$$Rh^{I}\text{---}\overset{O}{\underset{O}{\|}}$$

with the implication that the O_2 ligand has the ability to rotate in the manner of a propeller.

Activation parameters reported by Vaska and co-workers for the dissociation of O_2 from the complexes [Ir(X)(O_2)-

(20) Frech, C. M.; Shimon, L. J. W.; Milstein, D. *Helv. Chim. Acta* **2006**, *89*, 1730.

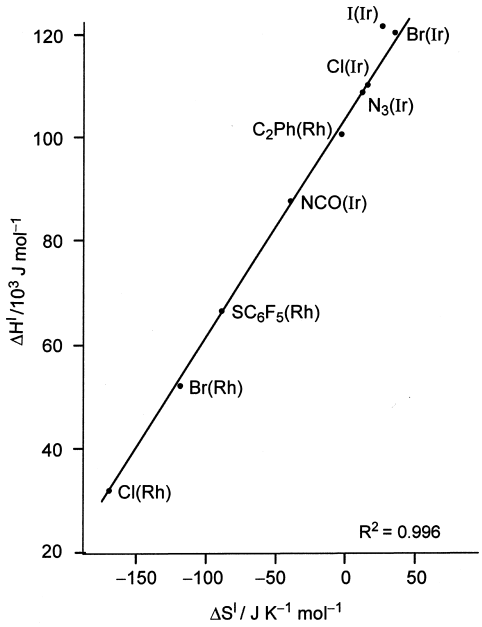

Figure 6. Plot of of $\Delta H^{\ddagger}$ vs $\Delta S^{\ddagger}$ for the dissociation of O_2 from $[Rh(X)(O_2)(XNC)(PPh_3)_2]$ (X = Cl, **5**; Br, **6**; SC_6F_5, **7**; C_2Ph, **8**) and from $[Ir(X)(O_2)(CO)(PPh_3)_2]$ (X = NCO, N_3, Cl, Br, I) in chlorobenzene. Data for the iridium complexes are taken from ref 18.

$(CO)(PPh_3)_2]$ (X = NCO, N_3, Cl, Br, I)[18] follow a similar pattern to those given here for $[Rh(X)(O_2)(XNC)(PPh_3)_2]$ (X = Cl, Br, SC_6F_5, C_2Ph) and are included in Figure 6 which shows that the plot of $\Delta H^{\ddagger}$ against $\Delta S^{\ddagger}$ for the rhodium complexes can be extended to include the iridium complexes (the data for the Ir iodide complex appear somewhat anomalous). The two series of complexes would therefore appear to share a common dissociation mechanism. Figure 6 shows that $\Delta H^{\ddagger}$ increases for the rhodium complexes in the sequence Cl < Br < SC_6F_5 < C_2Ph and for the iridium complexes in the sequence NCO < N_3 < Cl < Br with $\Delta H^{\ddagger}$ for the Cl- and Br-containing iridium complexes having significantly higher values than for the rhodium counterparts. Taking into account both series of complexes (Rh, Ir) an ordering of the anionic ligands according to their ability to enhance the binding of O_2 is NCO < N_3 < Cl < Br < SC_6F_5 < C_2Ph. For the rhodium complexes *trans*-$[Rh(X)(X\text{-}NC)(PPh_3)_2]$, a stable O_2 adduct is obtained with X = SC_6F_5 and with C_2Ph, (and not with Cl or Br). A stable O_2 adduct is also found for X = CN[16] indicating that an appropriate position for the CN ion in the above sequence is to the right of Br (i.e., Cl < Br < CN). The sequence of anionic ligands given above clearly reflects variations in an electronic property of the ligands X but does not match the ordering (taken in either direction) of the spectrochemical (Br < Cl < NCO < CN)[21] or nephelauxetic (CN ~ Cl < Br)[22] series; neither is there agreement with the ordering of ν_{co} for the complexes *trans*-$[Rh(X)(CO)(PPh_3)_2]$ (C_2Ph < Cl, Br < SC_6F_5)[23−25] where a low wavenumber is generally taken to indicate the presence of a good σ donor and/or poor π acceptor (but see also ref 26). The ordering of the anionic ligands derived from the data in Figure 6 can, however, be readily accounted for qualitatively in terms of their relative polarizability.

The ease or difficulty with which the electron density on a coordinatively unsaturated metal atom can be attracted to an approaching electrophile (a process in which the metal becomes electronically polarized) will reflect contributions both from the metal and from the ligands. The metal atom can be regarded as having a certain intrinsic polarizability which increases on moving down a group of the Periodic Table and on which are superimposed effects arising from variations in oxidation state and of ligands. A ligand may be polarizable by virtue of having a polarizable donor atom (Cl, Br, S) or as a consequence of having a multiply bonded π electron system (CN, C_2Ph), the polarizability being inversely proportional to the π-acidity of the ligand. Such a ligand can be regarded as possessing stored electron density that can be given up to the metal on demand, that is, when constrained to do so as a result of an interaction between the metal and an electrophile. The availability of this stored electron density will only be poorly reflected in spectroscopic measures of (relative) electron density on the metal in its ground-state but would be expected to become apparent in a situation involving electronic distortion of the metal induced by an external reagent such as O_2.

From this perspective the data in Figure 6 show, perhaps unsurprisingly, that iridium is intrinsically more polarizable than rhodium and that polarizable ligands enhance the binding of O_2 to the metal. In view of the high correlation between $\Delta H^{\ddagger}$ and $\Delta S^{\ddagger}$, strongly indicating a common pathway for the dissociation process, it becomes meaningful to attribute differences in these parameters to differences in polarizabilities of both the metal and the ligands. Although the contributions of the metal and the ligands are not entirely separable, it is possible from Figure 6 to conclude that the ligands show increasing polarizability in the order NCO < N_3 < Cl < Br < SC_6F_5 < C_2Ph, that their contribution to the polarizability of the respective Rh and Ir complexes is proportionately greater in the case of rhodium than of iridium, and that the influence on the activation parameters of changes in the polarizability of the anionic ligand is, to a good approximation, equivalent to that of changes in the intrinsic polarizability of the metal (i.e., of exchanging one metal for the other). This means that within the limits imposed by the present data the activation parameters are insensitive to the source of the electron density that is given up by the complex to the oxygen, that is, to the relative contributions made by the metal and by the anionic ligand. This is by no means an obvious result, and further work will help to establish how widely applicable it is likely to be.

Conclusion

Activation parameters for the dissociation of O_2 from the complexes $[Rh(X)(O_2)(XNC)(PPh_3)_2]$ show that the influence

(21) Cotton, F. A.; Wilkinson, G. *Advanced Inorganic Chemistry*, 3rd ed.; J. Wiley: London, 1972; p 577.
(22) Mason, J. *Chem. Rev.* **1987**, *87*, 1299.
(23) Cetinkaya, B.; Lappert, M. F.; McMeeking, J.; Palmer, D. E. *J. Chem. Soc., Dalton Trans.* **1973**, 1202.
(24) Vaska, L.; Peone, J. *J. Chem. Soc., Chem. Commun.* **1971**, 418.
(25) Carlton, L. *J. Organomet. Chem.* **1992**, *431*, 103.
(26) McAuliffe, C. A.; Pollock, R. *J. Organomet. Chem.* **1974**, *77*, 265.

of ligand X in stabilizing the O_2 adduct increases in the order Cl < Br < SC_6F_5 < C_2Ph. A high correlation between $\Delta H^{\ddagger}$ and $\Delta S^{\ddagger}$, in a plot which can be extended to include work of earlier researchers using complexes of iridium, can be taken as strong evidence of a common dissociation pathway for complexes [M(X)(O_2)(L)(PPh_3)$_2$] (M = Rh, L = XNC; M = Ir, L = CO) and a single reaction coordinate along which the rate-determining step occurs at a different position (indicated by the magnitude of $\Delta H^{\ddagger}$) for each relevant combination of M, X, and L. The comparison of properties of ligands X in terms of their respective contributions to $\Delta H^{\ddagger}$ (for given M and L) is then practicable. The influence of ligand X on $\Delta H^{\ddagger}$ can be related to its polarizability, that is, to the presence of electron density that in the unoxygenated complex resides on the ligand but which, in the presence of O_2, is given up to the metal to facilitate the metal−O_2 interaction. It is proposed that the sequence NCO < N_3 < Cl < Br < SC_6F_5 < C_2Ph represents a scale of increasing polarizability of the anionic ligand.

Acknowledgment. We thank the University of the Witwatersrand for financial support and Professor H.M. Marques for useful discussion.

Supporting Information Available: Crystallographic data in CIF format. This material is available free of charge via the Internet at http://pubs.acs.org.

IC800478G